Babylonian Journal of Mechanical Engineering
Vol.2024, **pp**. 64–70
DOI: https://doi.org/10.58496/BJME/2024/008; ISSN: 3006-5410
https://mesopotamian.press/journals/index.php/BJME

Research Article

Numerical Investigation of Grooved Obstacle on Heat Transfer Inside A Heated Duct

Jenan S. Sherza 1,*,
[1] *Department of Mechanical Engineering, University of Technology, Baghdad, Iraq.*

ARTICLE INFO

Article History
Received 17 May 2024
Revised: 17 Jun 2024
Accepted 18 Jul 2024
Published 12 Aug 2024

Keywords
Heated duct,
ribs,
turbulators,
turbulence augment,
vortex generators.

ABSTRACT

Flow and heat transfer are simulated numerically in a 2-dimensional centerline- ribbed square duct for different values of the rib height to the duct height (Blocking ratio BR). The blocking ratio of these rectangular obstacles 0, 0.5 and 0.75 are examined. Three values of velocity (0.1, 1 and 4m/s) as inlet working conditions were used. The top and bottom face of the duct are subjected to 1000 W/m2 heat flux. The heat transfer and flow structure with Ansys-Fluent inside a square duct in the presence of rotating vortex generators were studied and the influence of the blocking ratio (BR) on both heat transfer and fluid flow are examined. Numerical simulation was performed by using Ansys-Fluent 18. . In general, the enhancement raticon of heat transfer could reach 54%.

1. INTRODUCTION

Researchers and companies have taken care of enhancement of the work, performance and efficiency of the apparatus, equipment and engines. One of the most important enhancements or improvements is heat transfer enhancement. Heat transfer enhancement is by increasing of heat transfer rate or increasing heat transfer coefficient. It can be obtained by making or adding some additives to the part of the apparatus that needed to improve heat transfer rate or coefficient inside or outside it. Heat transfer can be enhanced by making or adding roughness or roughness elements, fins, wings, ribs, rods, winglets (half-wings vertical to the fin plane), or any interrupted surfaces or porous surfaces to improve convection, boiling or condensation.

Bergles and Webb [1] asserted that impediments enhance heat transport by disturbing the thermal boundary layer. The configuration of the barrier substantially influences its efficacy; for example, spherical obstacles generate less flow separation compared to flat obstacles, leading to more consistent heat transmission. Saha and Dutta [2] noted that impediments positioned at regular intervals inside ducts induce periodic turbulence, enhancing mixing and heat transmission. They observed that smaller impediments at the surface facilitate localized turbulence, hence improving heat transfer next to the duct walls. Obstacles may induce a substantial pressure decrease, particularly when oriented perpendicular to the flow. Prasad and Mullick [3] examined the trade-off and determined that streamlined features, such as airfoil-shaped components, reduce pressure loss while preserving superior thermal performance. Han et al. [4] shown that rib geometries, including triangular, square, and semi-circular profiles, significantly affect heat transport. Their investigations demonstrated that V-shaped ribs positioned upstream provide the greatest benefit owing to improved flow reattachment and consistency in heat transmission.

Karwa [5] examined the Rib Height-to-Pitch Ratio (e/P) and determined that appropriate rib spacing enhances heat transmission by promoting serial flow reattachment. Excessively proximate ribs result in flow stagnation, while excessively distant ribs diminish turbulence intensity. Ahmed and Zohir [6] investigated roughened ribs and found that enhanced roughness augments heat transport by elevating turbulence intensity. Nonetheless, this also increases pressure drop, necessitating a meticulous equilibrium. Esfahani et al. [7] investigated the interplay between perforated barriers and downstream ribs inside conduits. Their studies demonstrated that the introduction of upstream impediments considerably modifies the flow, hence strengthening the efficacy of the ribs in improving heat transmission. Perforated barriers provide

*Corresponding author. Jenan.s.sherza@uotechnology.edu.iq

partial flow diversion, minimizing pressure loss while preserving turbulence. Sharma et al. [8] demonstrated that the integration of perforated obstacles with triangular ribs resulted in a 20% enhancement in heat transmission relative to setups using solid obstacles. Khoshvaght-Aliabadi et al. [9] examined triangular, trapezoidal, and circular ribs, indicating that triangular ribs exhibit enhanced performance owing to less drag and efficient flow reattachment. Moreover, tilted impediments enhanced thermal performance by conforming to the principal flow direction. Wu and Tao [10] examined the impact of rib spacing and found that staggered rib designs enhance heat transmission compared to linear arrangements by breaking uniform flow patterns and facilitating improved mixing. Ali and Afify [11] used CFD to investigate ribbed ducts, determining ideal rib angles that minimized pressure losses and improved heat transmission. Zhou et al. [12] proposed that adjusting the size of obstacles and ribs might decrease pressure loss by 15% while maintaining heat transfer efficiency. Chandra et al. [13] examined hybrid configurations that integrate ribs with vortex generators. A 30% enhancement in heat transport was seen in comparison to independent rib configurations. Al-Dulaimi et al. [14] investigate the efficacy of vortex generators (VGs) in augmenting heat transmission in ducts. The research specifically examines the use of detached square vortex generators in square ducts and assesses their impact on heat transmission and pressure drop. It utilizes numerical simulations using ANSYS FLUENT to examine the impact of many variables, such as blocking ratios, the quantity of vortex generators, angles of attack, and aspect ratios, on heat transfer performance. Karwa [15] shown that an ideal rib height, typically between 0.1 and 0.2 of the duct height, achieves a compromise between increased turbulence production and an acceptable pressure decrease. The rib pitch, defined as the spacing between successive ribs, is a significant determinant. Zhang and Liu [16] performed studies using staggered and inline configurations of ribs and barriers. Their findings demonstrated that staggered configurations, in which barriers and ribs are offset, resulted in elevated Nusselt values. This arrangement optimized turbulence while minimizing excessive frictional losses. The upstream positioning of impediments, followed by ribs, modifies the flow, enabling the ribs to generate more efficient turbulence. Ali and Afify [17] used CFD simulations to enhance rib designs and obstacle locations. Simulations demonstrated that turbulence models, including k-ε and Reynolds-averaged Navier-Stokes (RANS), effectively capture large-scale flow characteristics and forecast heat transfer. They observed that Large Eddy Simulation (LES) may be essential for intricate geometries. Patel et al. [18] corroborated CFD findings with wind tunnel experiments. Particle Image Velocimetry (PIV) was used to record flow patterns, while thermal measurements were utilized to confirm temperature distributions. Their results validated that CFD could consistently forecast the performance of ribbed ducts, while underscoring the significance of precise boundary conditions and turbulence models.

An examination of the literature indicates a need for further enhancement and evaluation of novel vortex generators in thermal systems, owing to the extensive use of heat exchangers and air ducts in industrial applications. This study numerically investigates the impact of grooved obstacle on the hydro-thermal performance inside a square duct.

2. PHYSICAL MODEL

The software SolidWorks was utilized to construct the three-dimensional flow domain geometry. The primary method involves initially sketching with 2D drawings, followed by the usage of 3D tools to generate the whole geometry. The computational domain is defined by three sections with a square cross-section of 680 mm. The initial section is referred to as the entrance region, which spans a length of 420mm (equivalent to 10 times the hydraulic diameter, Dh) to guarantee that the flow is properly developed. The second zone is referred to as the test region. Both the top and bottom faces get a consistent flow of heat. The ribs are located inside this region. The exhaust region is the area that links the test region to the surrounding environment. This area serves as a barrier, protecting the test region from the influence of the surrounding environment. Figure (1) depicts the model. The diameter of the obstacle is 20 mm and 31.2 mm

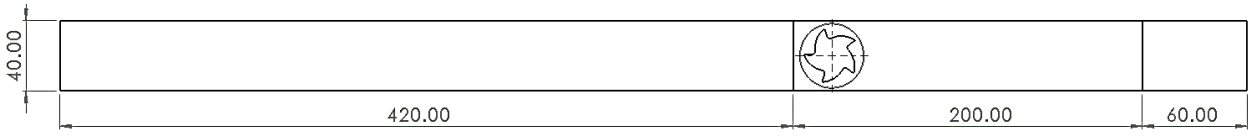

Fig. 1. The model

3. MESHING

Structured meshing is employed to mesh the entrance and exhaust sections due to their consistent section. Hexagonal elements are employed to create a mesh in these places. The test region is non-uniform due to the existence of obstacle; hence it is meshed using an unstructured approach. The mesh in this region was generated using tetrahedron elements.

The number of components has a substantial impact on the simulation results. In this study, the element number is crucial primarily in the test region, which encompasses fluid flow and heat transfer. To reduce the computational cost , suitable number of mesh elements must be determined carefully. Table (1) present the variation of the convective heat transfer coefficient ($\mathbf{h_{av}}$)inside the test section with element number. It can be seen the variation of the $\mathbf{h_{av}}$ is insignificant for all the tested elements number. The elements number is chose to be 50,589. Figure 2 depicts the meshed domain.

TABLE I. ELEMENTS NUMBER EFFECT ON THE AVERAGE HEAT TRANSFER COEFFICIENT WITH.

Elements number	h_{av}
28,524	87.9
34,218	88.24
50,859	88.259
77,478	88.26
28,524	88.262

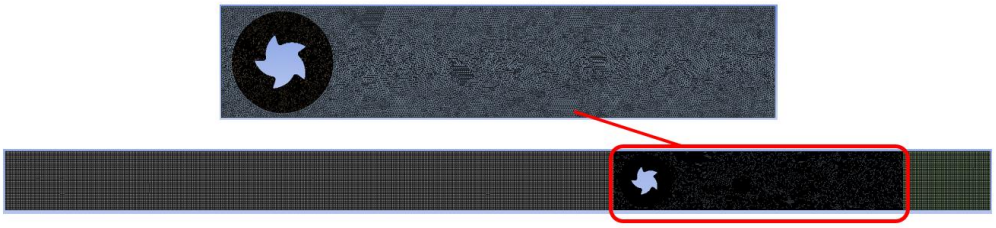

Fig. 2. The meshed domain

4. GOVERNING EQUATIONS

The Navier-Stokes equations, expressed in tensor notation, decompose variables into mean and fluctuation components through Reynolds averaging. This process resembles velocity decomposition [15]:

$$u_i = \bar{u}_i + u_i' \quad (1)$$

Where u_i is the instantaneous fluid velocity, u_i' is the velocity fluctuation and $\bar{u}_i$ is the time-averaged value of u_i at a point. The governing equations include: continuity, momentum and energy.

Continuity Equation

$$\frac{\partial \rho u}{\partial x} + \frac{\partial \rho v}{\partial x} + \frac{\partial \rho w}{\partial x} = 0 \quad (2)$$

The above equation may be expressed as follows, given that the mass density of fluid remains constant:

$$\frac{\partial u}{\partial x} + \frac{\partial v}{\partial x} + \frac{\partial w}{\partial x} = 0 \quad (3)$$

Then, the continuity equation is stated as:

$$\frac{\partial u_i}{\partial x_i} = 0 \quad (4)$$

Momentum Equation

$$\rho \frac{\partial u_i u_j}{x_j} = -\frac{\partial P}{\partial x_i} + \mu \frac{\partial}{\partial x_j}\left(\frac{\partial u_i}{\partial x_j} + \frac{\partial u_j}{\partial x_i}\right) + \rho \frac{\partial}{\partial x_j}(-\overline{u_i' u_j'}) \quad (5)$$

Energy Equation

$$\rho c_p \frac{\partial u_i T}{\partial x_i} = \frac{\partial}{\partial x_i}\left(\lambda \frac{\partial T}{\partial x_i} - \rho \overline{u_i' T'}\right) \quad (6)$$

Where λ : is thermal conductivity

Turbulence Model

Numerous turbulence models in Fluent are available to simulate diverse flow scenarios. The K-ε realizable model was used in this study. This model is advised [16] for flows characterized by vortices and rotation, such as those occurring inside ducts, including obstacles.

5. BOUNDARY CONDITIONS

The Governing equations are solved by utilizing the following boundary conditions as in Figure (3):

- Left edge: velocity inlet
- Right edge: pressure outlet.
- Test section: heat flux

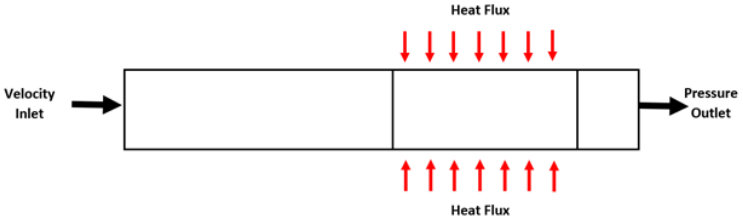

Fig. 3. The Boundary conditions

6. SOLUTION

In order to perform numerical simulations of the natural convection inside the annulus and between the glass cover and the surroundings, the ANSYS Fluent set-up, in detail described below, was chosen according to ANSYS recommendation **[14]**. The spatial discretization settings used for numerical simulations are the second order for all equations. The convergence criteria are set to 10^{-5} for all equations.

7. RESULTS

This study quantitatively examined heat transfer and flow structure inside a square duct, including circular ribs. This study analyzes the impact of the number of ribs (1, 2, 5, 7) and the placement angle θ (0, 30, 45 degrees). The ratio of rib height to duct height is 0.2. The convective heat transfer coefficient is calculated on the test section's top face. The average Nusselt number is then derived from the mean heat transfer coefficient.

7.1 Effect of Blocking Ratio

Figure (4) illustrates a relationship between the local heat transfer coefficient and the number of ribs inside the test section. The graphic demonstrates an improvement in the heat transfer coefficient as the number of ribs increases up to a particular threshold. This improvement is attributable to heightened turbulence levels as depicted in figure (5). . Figure (6) exhibits the enhancement trend of average Nusselt number due to the presence of the obstacle at the entrance of the test section. The enhancement reaches 52 % for inlet velocity 1m/s and 54% , and velocity 4m/s.

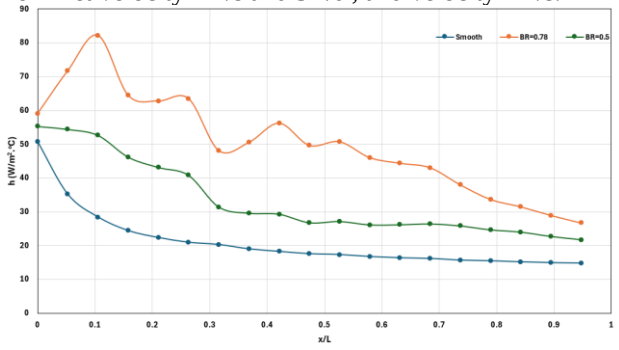

Fig. 4. Local heat transfer coefficient for different blocking ratios (V= 1m/s).

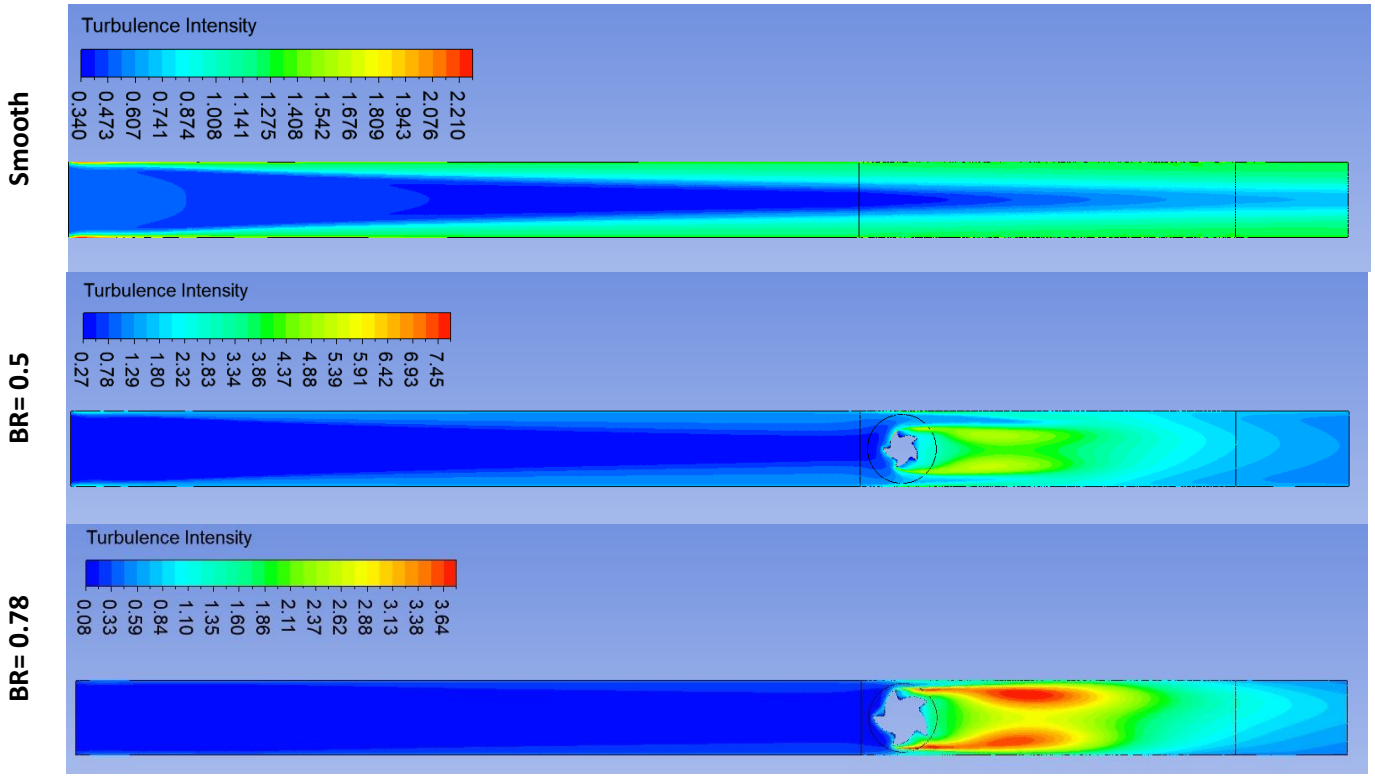

Fig. 5. Effect of blocking ration on turbulence distribution (V=1 m/s).

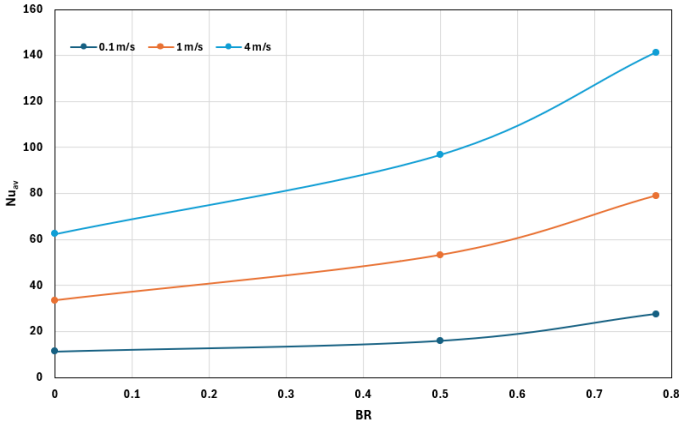

Fig. 6. Effect of velocity and blocking ration on average Nusselt number.

7.2 Effect of Blocking Ration on Pressure Drop

The influence of blocking ratio on pressure drop is shown in figure (7). It can be said that the relation is proportional. As the blocking ratio increases the flow cross section area decreases and more fluid is impeded, the pressure loss increases. The pressure drop of v =0.1 m/s is not presented in the figure 7 since it is less than 1.It can be noted that the pressure drop of case V=4 m/s is higher than that of V=1 m/s. This is due to the fact that as the higher velocity the higher kinetic energy of the flow which leads to higher loss in pressure when collision with the obstacle. Also, the pressure distribution inside the duct is shown in figure (8) for case of V= 1 m/s. It is obvious that the presences of the obstacle represents an opposite force on the flow and reduces its energy.

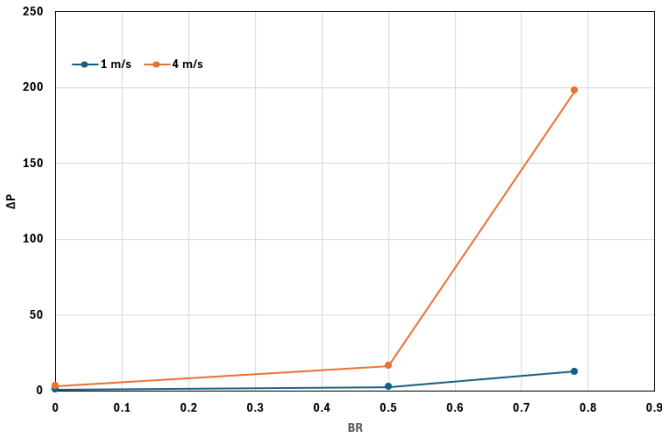

Fig. 7. Effect of velocity and blocking ration on pressure drop.

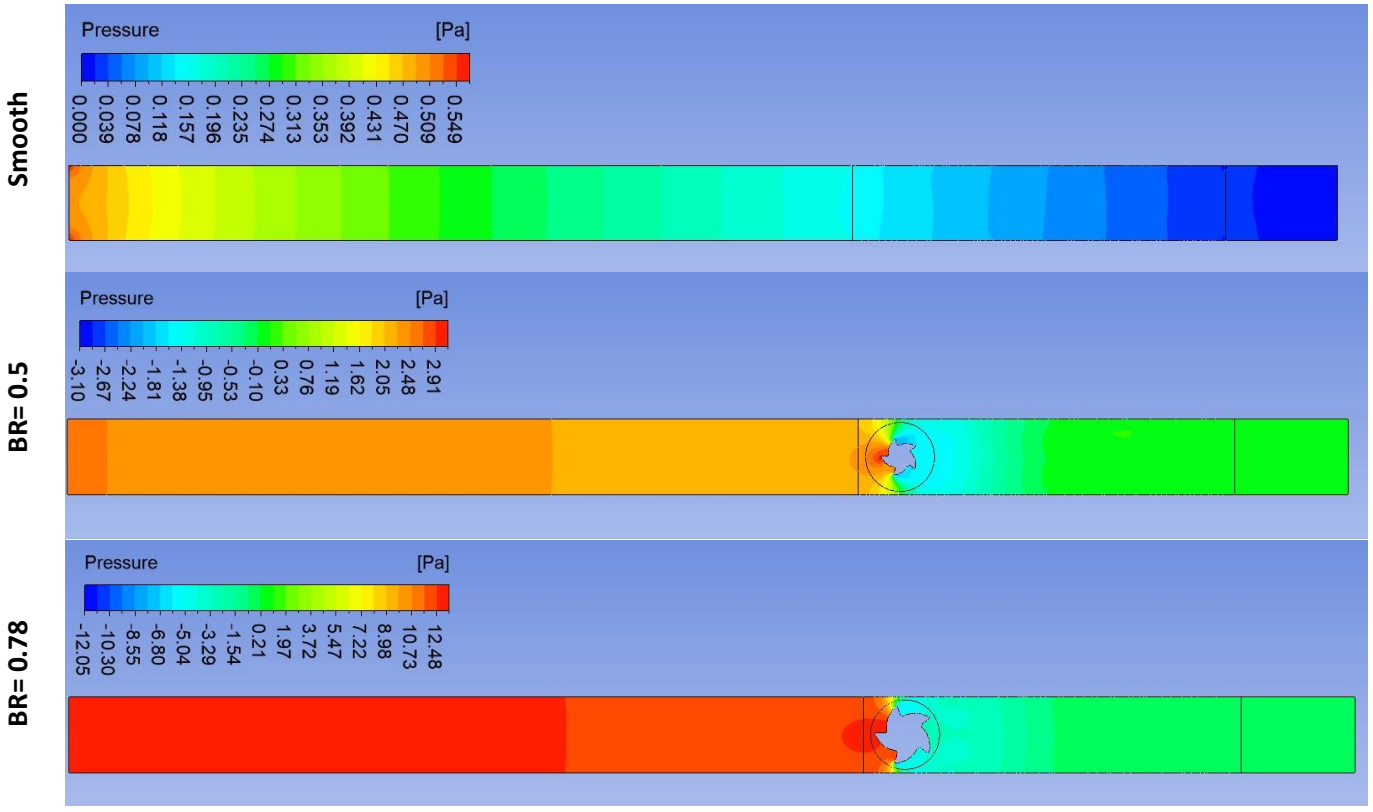

Fig. 9. Pressure distribution

8. CONCLUSIONS

A numerical analysis of the pressure drop and heat transfer properties in a heated square duct with a grooved obstacle installed at the test section was reported in this work. As inlet working conditions, three velocity values (0.1, 1, and 4 m/s) were used. The blocking ratio (BR) was set at 0, 0.5, and 0.75. To illustrate how ribs affect heat transport and pressure drop, the impact of these factors is examined. The current work's findings are as follows:

- Because of the increase in turbulence, the barrier generally has a favorable effect on heat transmission. The average heat transfer might be improved by up to 54%.
- As the blocking ratio rises, heat transfer tends to increase as well (until further limitations). For the case , BR=0.75, and a velocity of 1 m/s, the heat transfer improvement is 54%.

- It was determined that there is a proportionate relationship between the blocking ratio and pressure decrease. Pressure loss rises as the blocking ratio rises because the flow cross-section area shrinks and more fluid is obstructed.

Conflicts Of Interest

The author's paper explicitly states that there are no conflicts of interest to be disclosed.

Funding

The author's paper clearly indicates that the research was conducted without any funding from external sources.

Acknowledgment

The author acknowledges the institution for their commitment to fostering a research-oriented culture and providing a platform for knowledge dissemination.

References

[1] R. Bergles and R. Webb, "Obstacles improving heat transfer by disrupting the thermal boundary layer," J. Heat Transfer, vol. 107, no. 2, pp. 493-498, 1985.
[2] S. Saha and S. Dutta, "Effect of periodic obstacles on heat transfer in ducts," Int. J. Heat Mass Transfer, vol. 59, pp. 1234-1243, 2016.
[3] R. Prasad and S. Mullick, "Streamlined obstacles for heat transfer enhancement," J. Heat Transfer Eng., vol. 40, no. 7, pp. 629-639, 2018.
[4] Z. Han, S. Zhang, and L. Yang, "The effect of rib geometries on heat transfer enhancement in ducts," Heat Transfer Eng., vol. 34, no. 2, pp. 151-160, 2013.
[5] S. Karwa, "Effect of Rib Height-to-Pitch Ratio on heat transfer in ducts," Int. J. Thermal Sciences, vol. 42, pp. 733-744, 2003.
[6] S. Ahmed and A. Zohir, "Effects of rib roughness on heat transfer enhancement," Energy Conversion and Management, vol. 159, pp. 61-70, 2018.
[7] A. Esfahani, H. Najafi, and R. Jafari, "Interaction between perforated obstacles and downstream ribs in ducts," Int. J. Heat Mass Transfer, vol. 135, pp. 104-112, 2020.
[8] A. Sharma, S. Patil, and P. Desai, "Effect of perforated obstacles on heat transfer in ribbed ducts," J. Therm. Sci. Eng. Appl., vol. 13, no. 4, pp. 041012, 2021.
[9] M. Khoshvaght-Aliabadi, M. R. Tavakkol, and M. Zeynali, "Comparison of different rib geometries for heat transfer enhancement," Appl. Therm. Eng., vol. 144, pp. 465-473, 2019.
[10] L. Wu and J. Tao, "Analysis of rib spacing and configuration on heat transfer enhancement," Int. J. Heat Mass Transfer, vol. 106, pp. 259-269, 2017.
[11] R. Ali and H. Afify, "CFD study on ribbed ducts and optimal rib angles for heat transfer enhancement," Comput. Fluids, vol. 216, pp. 1045-1055, 2021.
[12] X. Zhou, J. Zhang, and L. Cheng, "Optimizing obstacle and rib dimensions for reduced pressure drop and enhanced heat transfer," Heat Transfer Eng., vol. 37, no. 6, pp. 453-462, 2016.
[13] S. Chandra, A. Sharma, and A. Prakash, "Hybrid designs combining ribs and vortex generators for heat transfer enhancement," Int. J. Therm. Sci., vol. 162, pp. 106481, 2023.
[14] M. J. Al-Dulaimi, F. A. Kareem, and F. A. Hamad, “Numerical investigation of the heat transfer enhancement inside a square duct with rectangular vortex generators,” J. Therm. Eng., vol. 8, pp. 1–13, 2022.
[15] S. Karwa, "Optimal rib height and pitch for maximum heat transfer in ducts," Heat Transfer Eng., vol. 24, no. 6, pp. 51-58, 2003.
[16] Y. Zhang and Y. Liu, "Effect of staggered and inline rib configurations on heat transfer," J. Fluids Eng., vol. 141, no. 9, pp. 091602, 2019.
[17] R. Ali and H. Afify, "CFD simulations of rib configurations and obstacle placements for heat transfer enhancement," Int. J. Therm. Sci., vol. 128, pp. 195-210, 2021.
[18] D. Patel, M. Kumar, and S. Joshi, "CFD validation of ribbed ducts using Particle Image Velocimetry," Exp. Therm. Fluid Sci., vol. 116, pp. 124-136, 2020.